Biotechnology Journal
www.biotechnology-journal.com

Biotechnol. J. 2015, 10

DOI 10.1002/biot.201400168

Review

Single-walled carbon nanotubes as near-infrared optical biosensors for life sciences and biomedicine

Astha Jain[1], Aida Homayoun[2], Christopher W. Bannister[1], and Kyungsuk Yum[1]

[1] Department of Materials Science and Engineering, University of Texas, Arlington, USA
[2] Department of Bioengineering, University of Texas, Arlington, USA

Received 16 JUL 2014
Revised 26 NOV 2014
Accepted 02 JAN 2015

Single-walled carbon nanotubes that emit photostable near-infrared fluorescence have emerged as near-infrared optical biosensors for life sciences and biomedicine. Since the discovery of their near-infrared fluorescence, researchers have engineered single-walled carbon nanotubes to function as an optical biosensor that selectively modulates its fluorescence upon binding of target molecules. Here we review the recent advances in the single-walled carbon nanotube-based optical sensing technology for life sciences and biomedicine. We discuss the structure and optical properties of single-walled carbon nanotubes, the mechanisms for molecular recognition and signal transduction in single-walled carbon nanotube complexes, and the recent development of various single-walled carbon nanotube-based optical biosensors. We also discuss the opportunities and challenges to translate this emerging technology into biomedical research and clinical use, including the biological safety of single-walled carbon nanotubes. The advances in single-walled carbon nanotube-based near-infrared optical sensing technology open up a new avenue for in vitro and in vivo biosensing with high sensitivity and high spatial resolution, beneficial for many areas of life sciences and biomedicine.

Keywords: Nanobiosensors · Nanobiotechnology · Near-infrared fluorescence · Optical biosensors · Single-walled carbon nanotubes

1 Introduction

Recent advances in nanobiotechnology have offered new opportunities for imaging, sensing, and therapeutics at the molecular level. Nanomaterials having a size comparable to biological macromolecules (1–100 nm) and unique physical and biological properties can transport diagnostic and therapeutic agents to target areas through nanoscale biological barriers, mediate molecular interactions, and detect target molecules for diagnostics and therapeutics [1]. Among nanomaterials, single-walled carbon nanotubes (SWNTs), with their extraordinary mechanical, electrical, thermal, and optical properties, have played an important role in this development [2–6].

SWNTs have attractive optical properties for life science and biomedical applications. Their quasi-one dimensional nanoscale structure provides SWNTs with intrinsic near-infrared (NIR) fluorescence (900–1400 nm) within the tissue transparency window, in which the biological tissue is optically transparent, ideal for their applications in biological environments (e.g., biological fluids, cells, and tissue). Their fluorescence is also nonphotobleaching, ideal for long-term sensing and imaging. Since the discovery of the NIR fluorescence of SWNTs, many research laboratories have explored how to use such extraordinary optical properties of SWNTs to develop nanoscale agents for biological imaging, sensing, and

Correspondence: Prof. Kyungsuk Yum, Department of Materials Science and Engineering, 501 West First Street, 329 Engineering Laboratory, Arlington, TX 76019
E-mail: kyum@uta.edu

Abbreviations: ATP, adenosine 5′-triphosphate; **BA-PhO-Dex**, boronic acid-phenoxy-dextran; **DAP,** diaminophenyl; **ELISA**, enzyme-linked immunosorbent assay; **FL,** Fluorescence; **MWNT**, multi-walled carbon nanotube; **NIR**, near-infrared; **NIR-II**, second near-infrared; **NO,** nitric oxide; **PEG**, polyethylene glycol; **PL**, photoluminescence; **QY,** quantum yield; **RBM**, radical breathing mode; **RES,** reticuloendothelial system; **RITC,** rhodamine isothiocyanate; **SNP**, single nucleotide polymorphism; **ssDNA**, single-stranded DNA; **SWNT**, single-walled carbon nanotube

photothermal therapeutics with new capabilities, unattainable with conventional fluorophores [2–6]. The ability to selectively modulate the fluorescence of SWNTs, for example, has led to the development of various NIR fluorescence-based SWNT sensors. SWNTs have several advantages as optical biosensors, including photostable NIR fluorescence for prolonged sensing in biological environments, particularly ideal for in vivo sensing. Furthermore, the high sensitivity of SWNTs to their local physical and chemical environments, including the adsorption of molecules, enables detection of analytes at the single-molecule level.

In this review, we present the recent advances in SWNT-based optical sensing technology for life sciences and biomedicine. We first introduce the electronic and optical properties of SWNTs, with emphasis on their second NIR (NIR-II) fluorescence for optical biosensing. We next discuss the mechanisms for molecular recognition and signal transduction in SWNT complexes. We then present the recent development of various SWNT-based NIR optical biosensors. Finally, we discuss the challenges and opportunities for the future development of the SWNT sensing technology, including the biological safety of SWNTs for biomedical research and clinical use [3, 6].

2 Structure and optical properties of single-walled carbon nanotubes

Carbon nanotubes are a high-aspect ratio nanostructure of sp^2-hybridized carbon atoms, conceptually constructed by rolling up graphene sheets into cylindrical tubes at a chiral angle (Fig. 1) [7–9]. The number of the layers of the graphene sheets classifies carbon nanotubes into single-walled carbon nanotubes (SWNTs; single layer of graphene) and multi-walled carbon nanotubes (MWNTs; multiple layers of graphene). SWNTs are a quasi-one-dimensional wire with diameters of 0.4–2 nm and lengths

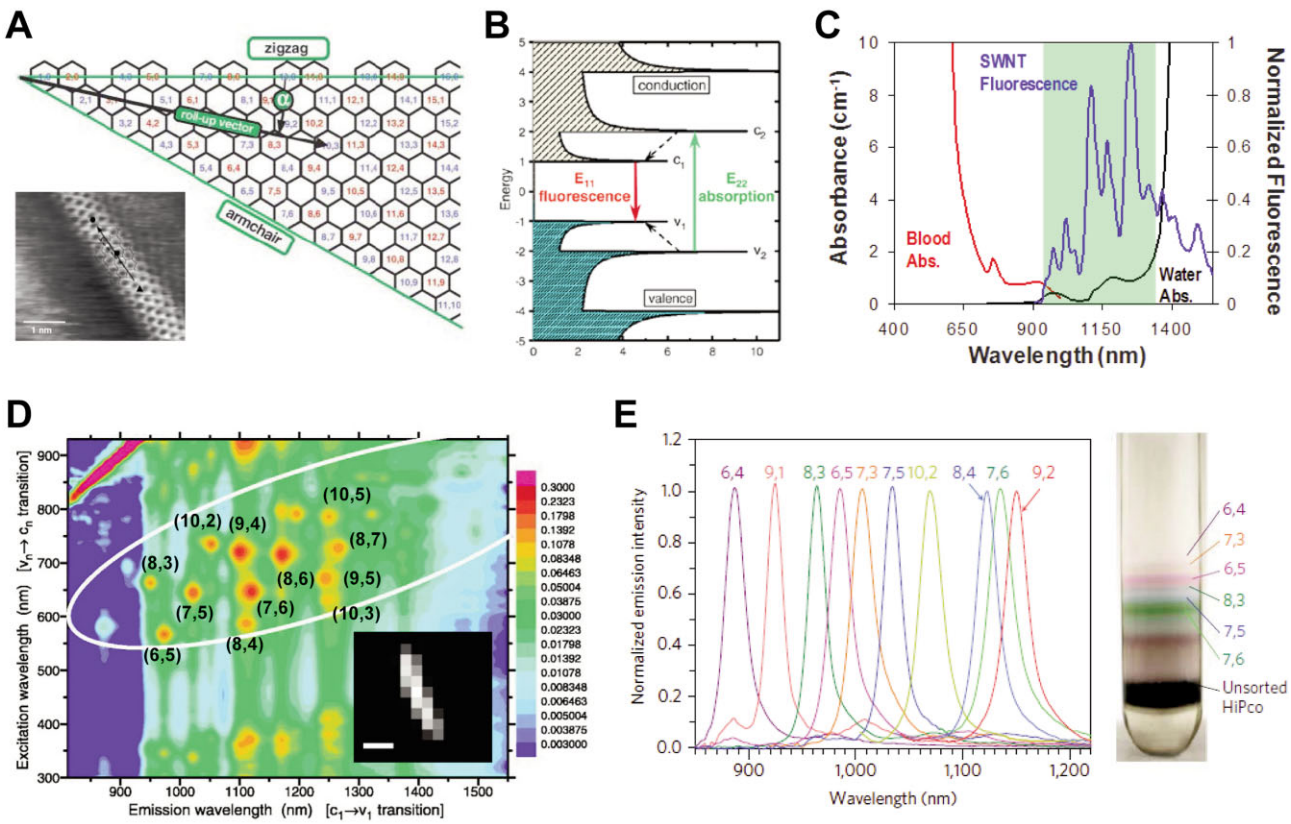

Figure 1. Structure and optical properties of single-walled carbon nanotubes (SWNTs). (**A**) Schematic of a graphene sheet showing a roll-up vector and a chiral angle (α) to form a SWNT [12] and scanning tunneling microscopy image of a SWNT (inset) [8]. SWNTs designated (n, m) are conceptually constructed by rolling a graphene sheet from (0, 0) to (n, m) along the roll-up vector. (**B**) Electronic density of states of semiconducting SWNTs with van Hove singularities [12]. Solid arrows show the optical excitation (E_{22}) and emission (E_{11}) transitions. Dashed arrows indicate nonradiative relaxation of the electron and hole before emission. (**C**) Fluorescence of SWNTs at NIR wavelengths (shown in blue) within the tissue transparency window, in which the absorption of biological tissues is minimal, bounded by blood (shown in red) and water (shown in black) absorption [4]. (**D**) Fluorescence intensity versus excitation and emission wavelengths of SWNTs [12]. (**E**) Fluorescence spectra of 10 separated (n, m) SWNT species excited at the E_{22} peak (left) and separated SWNTs by (n, m) structure using single-step nonlinear density-gradient ultracentrifugation (right) [13]. The distinct color bands show layers of enriched (n, m) SWNT species. Reproduced from [4, 8, 12, 13] with permission.

of up to several centimeters (Fig. 1A). This quasi-one-dimensionality renders sharp peaks in the electronic density of states (van Hove singularities; Fig. 1B) [10–12]. This electronic structure of SWNTs provides unique electronic and optical properties. Semiconducting SWNTs absorb light at photon energy E_{22} and emit fluorescence at E_{11} in the NIR range of 900–1600 nm (Fig. 1B and C) [4, 11]. The values of E_{11} and E_{22} vary with the chiral structure of SWNTs, designated by the roll-up vector (n, m) that defines the direction along which a graphene sheet is rolled to form a SWNT (Fig. 1A). Therefore, semiconducting SWNTs with different (n, m) structures, thus with different diameters, emit fluorescence at different wavelengths (Fig. 1D and E) [11, 13]. SWNTs with $n - m = 3k$, where k is an integer, are metallic or semimetallic and do not fluoresce [11]. Although MWNTs emit fluorescence at visible wavelengths [14, 15], we will confine our discussion to the use of the NIR band gap fluorescence of semiconducting SWNTs for biosensing [11]. With their larger sizes, MWNTs can function as a complementary platform for different biological applications, including intracellular delivery of large biomolecules (e.g., DNA plasmids) [16–22].

The optically excited states of semiconducting SWNTs are excitonic (i.e., form electron–hole pairs) [23, 24]. The excitons have binding energies of up to ~0.5 eV (e.g., 0.4 eV for 0.8-nm SWNTs with the band gap energy of 1.3 eV) [23], exciton sizes of a few nanometers [25], and exciton diffusional ranges of 100–300 nm [26, 27]. The excitonic nature of optically excited states of SWNTs provides a highly sensitive mechanism to modulate the fluorescence of SWNTs through external perturbations (as further discussed in Section 4) [23].

In addition to NIR fluorescence, SWNTs show strong resonance Raman scattering [28–33]. The resonance Raman excitation at the optical transitions (e.g., E_{11} and E_{22} transitions) significantly enhances the Raman scattering signals of SWNTs (i.e., resonance enhancement). The Raman scattering of SWNTs thus varies with their diameters and chiral structures [34]. SWNTs have multiple Raman scattering peaks, which arise from the different vibration modes of SWNTs, including radical breathing mode (RBM; 100–300 cm^{-1}) and tangential mode (G band; ~1580 cm^{-1}) [33, 34]. These Raman peaks are intense and narrow, with a full width at half-maximum of less than 2 nm, ideal for multiplexing sensing and imaging and easy to detect in biological environments with high autofluorescent backgrounds [30, 32, 33].

3 NIR fluorescence of SWNTs for optical biosensing

The inherent optical properties of SWNTs offer unique opportunities for optical biosensing (Fig. 1). First, SWNTs fluoresce at NIR wavelengths (900–1600 nm; Fig. 1C). This wavelength range is within the "tissue transparency window," in which the optical absorption of biological tissues is minimal, bounded by hemoglobin and water absorption (Fig. 1C) [35, 36]. SWNT-based optical biosensors operated at these NIR wavelengths could outperform conventional optical biosensors operated at visible wavelengths (particularly for in vivo sensing), because blood, cells, and tissues are strongly absorbing and autofluorescent at visible wavelengths. Second, the fluorescence of SWNTs does not photobleach [28], and the intensity of the fluorescence does not fluctuate [37]. Thus, SWNT-based sensors could persist indefinitely, ideal for long-term sensing. In comparison, most conventional fluorophores emit fluorescence at visible wavelengths and rapidly photobleach, limiting their applications. In this section, we discuss three figures of merit for fluorescence-based biosensors using SWNTs: signal intensity (quantum yield) in biological media, tissue penetration depth (NIR-II fluorescence) for in vivo sensing, and photostability for real-time, long-term sensing.

3.1 High signal intensity in the biological medium

The intensity of the optical signal of sensors is a critical constraint for the design of optical sensors. For biosensing, both the quantum yield of fluorophores and the optical absorption in the biological environment (e.g., biological media, cells, and tissues) determine the intensity of the optical signal. The quantum yield is the ratio of the number of photons emitted to the number of photons absorbed upon excitation. Because the optical absorption varies with wavelengths, the intensity of the optical signal emitted by a sensor that can be measured by a detector I_S strongly depends on the wavelength of the excitation light and the emitted light: $I_S = I_0 \phi e^{-2\mu d - k\tau}$, where I_S is the time-dependent intensity of the fluorescence signal, I_0 is the intensity of the incident light, ϕ is the quantum yield, μ is the absorption coefficient, which varies with the wavelength, d is the distance from the surface of the biological medium (e.g., tissue) to the sensor, k is the pseudo-first-order photobleaching rate constant, and τ is the aggregate excitation exposure lifetime [38]. Table 1 shows the estimated values of the apparent quantum yield $\phi e^{-2\mu d}$ (i.e., I_S/I_0 or the optical signal that can be detected outside the human body for a given incident excitation without considering photobleaching) for common fluorophores and SWNTs [38]. Despite the high quantum yield, the high absorption significantly attenuates the fluorescence signal at visible wavelengths; therefore, the apparent quantum yield of NIR fluorophores and SWNTs are significantly higher than that of visible fluorophores (Table 1). We also note that the quantum yield of SWNTs can be as high as 20% [39–41]. The low autofluorescent backgrounds of biological cells and tissues at NIR wavelengths further benefit NIR sensing, increasing the signal-to-noise ratio.

Table 1. Comparison of the apparent quantum yield (QY) of visible and NIR fluorophores in the human whole blood, a dominant absorber in the human body. Reproduced from [38] with permission.

Fluorescent probes	QY (%)	Conditions for QY measurement	Excitation (nm)	μ (oxygenated)	μ (deoxygenated)	Apparent QY ($\phi e^{-2\mu d}$)[a]
Cy5	27	PBS	620	2	60	3.20×10^{-28}
Fluorescein	95	0.1 M NaOH	496	150	120	5.23×10^{-118}
Rhodamine 6G	95	Water	488	200	105	3.30×10^{-133}
Rhodamine B	31	Water	514	110	190	1.60×10^{-131}
Indocyanine green	0.266	Water	820	0.96	0.77	4.72×10^{-4}
Indocyanine green	1.14	Blood	830	1.01	0.78	1.91×10^{-3}
Type II NIR QD	13	PBS	840	1.05	0.78	2.09×10^{-2}
SWNT	1[b]	PBS	1042	0.889	0.12	3.65×10^{-3}

QY, quantum yield; PBS, phosphate-buffered saline; QD, quantum dot.
a) Calculated using $d = 1$ cm and an average μ.
b) The QY of SWNTs can be as high as 20% [39–41].

3.2 Optical tissue penetration for in vivo sensing

Optical penetration depth assesses the performance of optical sensors more completely than absorption alone (or the apparent quantum yield) for in vivo sensing, because both scattering and absorption attenuates the optical signal. Optical penetration depth is defined as $\delta = (3\mu_a(\mu_a + \mu'_s))^{-1/2}$, where μ_a is the absorption extinction coefficient and μ'_s is the reduced scattering coefficient [35]. Because of the inverse dependence of scattering on the wavelength ($\mu'_s \approx \lambda^{-w}$, where λ is the wavelength and the exponent w varies with the type of tissues in the range of 0.22–1.68), the penetration depth of visible fluorophores is significantly reduced by scattering in tissue [35, 42]. Among NIR fluorophores, experimental and modeling studies show that the penetration depth can be maximized in the range of wavelength of 1000–1400 nm (named the second NIR window or NIR II window) [35, 42–45].

3.3 NIR-II fluorescence for high-resolution in vivo sensing

SWNTs fluoresce at NIR-II wavelengths (900–1400 nm) upon excitation at NIR-I wavelengths (700–900 nm), whereas most conventional NIR fluorophores fluoresce at NIR-I wavelengths (700–900 nm). Compared to the conventional NIR-I window, the longer wavelength emission of SWNTs in the NIR-II window have inherent advantages for in vivo imaging and sensing, due to reduced adsorption [46, 47], reduced scattering ($\mu'_s \approx \lambda^{-w}$) [35, 44], and negligible autofluorescence (thus, higher penetration depth in the tissue) [35, 45, 48].

Dai and coworkers [35, 45] compared the effects of scattering and absorption on the optical signal of indocyanine green and IRDye-800 (NIR I) and SWNTs (NIR II). SWNTs (NIR II) better preserve image clarity and contrast with increased depth than NIR-I fluorophores. They also demonstrated the use of the NIR-II fluorescence of SWNTs for epifluorescence imaging of vascular structures with high spatial (~30 μm) and temporal (<200 ms per frame) resolution at 1–3 mm deep in the hind limb of a mouse, unattainable by conventional NIR-I fluorophores [45]. The images obtained from the NIR-II fluorescence of SWNTs show a significantly improved image contrast and spatial resolution. Another advantage of SWNTs (NIR II) over NIR-I fluorophores is low autofluorescence (i.e., higher signal-to-background noise ratio), due to longer excitation (NIR-I) and emission (NIR-II) wavelengths of SWNTs than NIR-I fluorophores and large Stokes shifts of SWNTs (up to ~400 nm). The unique NIR-II fluorescence of SWNTs also benefits other in vivo applications, including tumor detection [33, 45, 49–55] and photothermal treatment [2, 50, 52, 56].

3.4 Photostability for long-term sensing

The photostability of fluorophores is a limiting factor that determines the lifetime of optical sensors. SWNTs are nonphotobleaching, ideal for real-time long-term sensing [28, 36, 38]. For instance, assuming an error tolerance of 20%, a simple calculation using the time-dependent intensity of the sensor signal, $I_S = \phi e^{-2}\mu^{d-k}\tau$, estimates the lifetime of a sensor to be $\tau = -\ln(0.8/k)$ [38]. This calculation estimates the lifetime of fluorescence sensors that use Cy5, ICG, and NIR QD to be 39.1 seconds, 5.4 h, and 2.7 h with the photobleaching rate constant k of 20.52, 0.0412, and 0.0827 h^{-1}, respectively, whereas SWNTs persist indefinitely [38].

4 Sensing mechanisms: Signal transduction and molecular recognition

The two main challenges in sensor design are molecular recognition and signal transduction [57]. The ability to modulate the fluorescence of SWNTs through external perturbations makes SWNTs unique nanoscale platforms

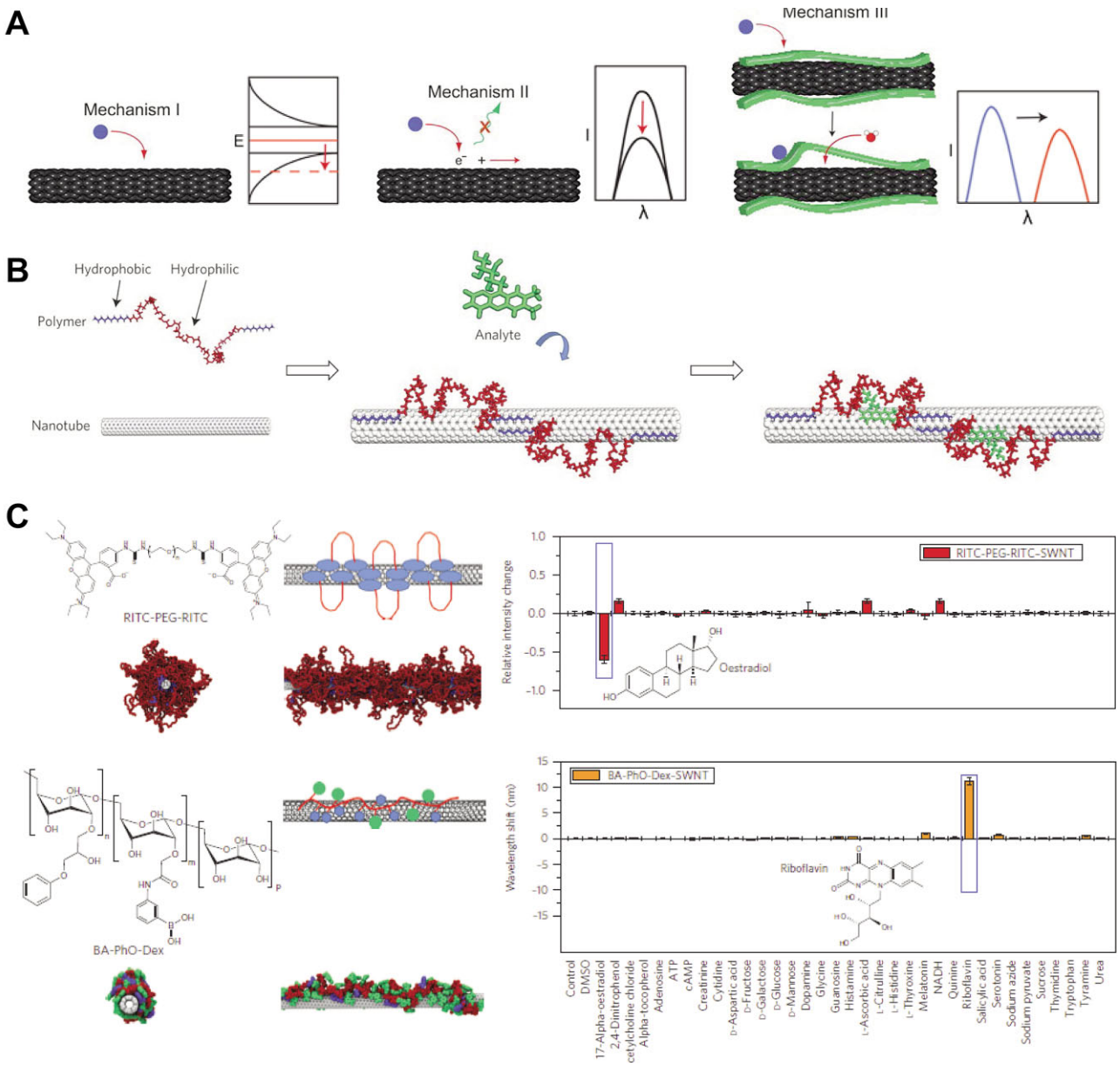

Figure 2. Signal transduction and molecular recognition in SWNT complexes. (**A**) Representative mechanisms for the modulation of the fluorescence of SWNTs, using charge-transfer (mechanisms I and II) and solvatochromism (mechanism III) [61]. (**B**) Schematic of the molecular recognition concept using corona phase complexes on SWNTs [57]. An amphiphilic polymer adopts a specific conformation when adsorbed on the surface of a SWNT. The polymer constrained on the surface of the nanotube creates a selective molecular recognition site for a specific molecule. The binding of the molecule on the molecular recognition site leads to a change of the wavelength or intensity of SWNT fluorescence. (**C**) Selective recognition of oestradiol using Rhodamine isothiocyanate-difunctionalized poly(ethylene glycol)–SWNT complexes (RITC-PEG-RITC–SWNTs; top) and riboflavin using boronic acid substituted phenoxy-dextran-wrapped SWNT complexes (BA-PhO-Dex–SWNTs; bottom). RITC-PEG-RITC–SWNTs and BA-PhO-Dex–SWNTs selectively recognize oestradiol via fluorescence quenching and riboflavin via wavelength shift, respectively. The polymer structures (top left), schematics (top right) and front (bottom left) and side (bottom right) views, obtained from molecular dynamics simulations, of the polymer–SWNT complexes, are shown to the left of the bar charts. The bar charts show the change of the fluorescence of the complexes against a panel of 36 biological molecules. (D) BA-PhO-Dex–SWNT sensors for spatial and temporal imaging of riboflavin live Raw 264.7 macrophage cells. Bright-field and NIR fluorescence of BA-PhO-Dex–SWNT complexes inside the macrophage cell (left) and time-evolution images showing the redshift of the emission wavelength of the sensors inside the cell upon addition of extracellular riboflavin (right). Reproduced from [57, 61] with permission.

for NIR optical sensing. Because all atoms of SWNTs are on the surface, SWNTs are highly sensitive to their local physical and chemical environment and surface adsorption events, even allowing for the detection of single molecules [26, 58–60]. In this section, we discuss the mechanisms for the selective modulation of SWNT fluorescence

(signal transduction) and molecular recognition in SWNT complexes for optical biosensing.

4.1 Signal transduction: Selective modulation of fluorescence

Figure 2A shows major mechanisms to modulate the fluorescence of SWNTs [61]. First, adsorption of redox-active molecules with a favorable reduction potential to the surface of SWNTs induces electron transfer between SWNTs and adsorbed molecules (mechanisms I and II in Fig. 2A) [58, 59, 62–67]. The electron transfer affects the fluorescence spectrum of SWNTs via bleaching of the electronic transition (via ground-state electron transfer; mechanism I in Fig. 2A) [63, 64, 66] or quenching of excitons (via excited-state electron transfer; mechanism II in Fig. 2A) [64, 65, 67], depending on the potentials of SWNTs and the adsorbed molecules (thus depending on the chirality of SWNTs) [63–67]. The reversible nature of the bleaching and quenching also allows for a "turn-on" sensing scheme that uses the recovery of the reduced fluorescence upon binding of analytes [63–65, 67]. Second, the change of the local dielectric environment around SWNTs causes solvatochromic shift (mechanism III in Fig. 2A) [68–70]. The adsorption of analytes changes the dielectric environment directly by replacing solvent molecules or indirectly by perturbing the conformation of polymers that wraps around SWNTs. An example is ion-induced conformational transitions of DNA secondary structures in DNA-wrapped SWNTs that induces a red shift of the fluorescence of SWNTs [71, 72]. In many cases, the combination of these mechanisms modulates the fluorescence of SWNTs [36, 64].

4.2 Molecular recognition

Engineering SWNT complexes can incorporate molecular selectivity into the above discussed mechanisms for signal transduction [61]. Direct engineering of polymer-encapsulated SWNT complexes (both the polymers themselves and the interface between the polymers and the nanotubes) can incorporate molecular selectivity into SWNT complexes [57]. For example, Zhang et al. [57] demonstrated molecular recognition using corona phase complexes on SWNTs (Fig. 2B) [57]. In this work, engineered synthetic heteropolymers constrained on the surface of SWNTs create corona phase complexes that selectively recognize specific molecules through the combination of analyte adsorption to the surface of SWNTs and lateral interactions with molecules in the adsorbed phase, resulting in modulation of the fluorescence of SWNTs (Fig. 2B). To prove this phenomenon, they demonstrated three examples of heteropolymer–nanotube recognition complexes for oestradiol, riboflavin, and L-thyroxine and the prediction of recognition using a thermodynamic model of surface interactions (Fig. 2C). They also demonstrated that the complexes can be used as a spatiotemporal NIR optical sensor, as shown by tracking riboflavin diffusion in murine macrophages (Fig. 2D) [57]. Kruss et al. [73] also extended this approach to detect neurotransmitters. Another strategy is to use conventional molecular recognition entities, such as enzymes [64, 74], oligonucleotides [75, 76], aptamers [77, 78], and proteins [79, 80]. Examples include SWNT-based NIR optical sensors for proteins, small molecules, and glucose (as further discussed in Section 5) [64, 67, 74–81].

Because SWNTs with different chiral structures respond to the adsorption of molecules spectroscopically differently (due to their different electronic structures), SWNTs can function as a multimodal sensor. For example, Heller et al. [59] demonstrated multiplexed optical detection of genotoxic analytes using (6, 5) and (7, 5) nanotubes. The recent advances in the single-chirality separation of SWNTs would fully realize the potential for multiplexed sensing [13, 51, 52, 82–86].

5 SWNT-based NIR optical biosensors

Many researchers have used the above discussed mechanisms for molecular recognition and signal transduction to develop various SWNT-based NIR optical biosensors. In this section, we present examples of SWNT sensors for DNA (detection of DNA structures and sequences), proteins and small molecules (Fig. 3). We also include sensors that use SWNTs as NIR labels [87]. Table 2 summarizes these sensors.

5.1 Early development: Detection of DNA structures and sequences

DNA-wrapped SWNTs are one of the earliest examples of SWNT sensors. DNA-wrapped SWNTs directly detect DNA hybridization [75, 76], single nucleotide polymorphism (SNP) [88], and conformational polymorphism [71, 72] using the solvatochromic shift [68–70]. For example, Jeng et al. [75, 76] demonstrated the optical detection of DNA hybridization using single-stranded DNA (ssDNA)-wrapped SWNTs. Hybridization of ssDNA on the ssDNA-wrapped SWNTs with its complement induces a hypsochromic shift of 2 meV with the detection limit of 6 nM. In this hybridization process, an increase in the coverage of DNA on the surface of SWNTs changes the local dielectric environment, inducing the solvatochromic shift. The high sensitivity of DNA-wrapped SWNTs also enables the differentiation of single nucleotide polymorphism through the solvatochromic shift from that of a full complementary strand [88]. Heller et al. [71] also studied the metal ions-induced transition of DNA conformations from the B-form to Z-form on the surface of DNA-wrapped SWNTs, which changes the dielectric environment around the SWNTs. Using this mechanism, they demonstrated the detection of divalent metal ions (e.g., Hg^{2+}) in whole blood, tissue,

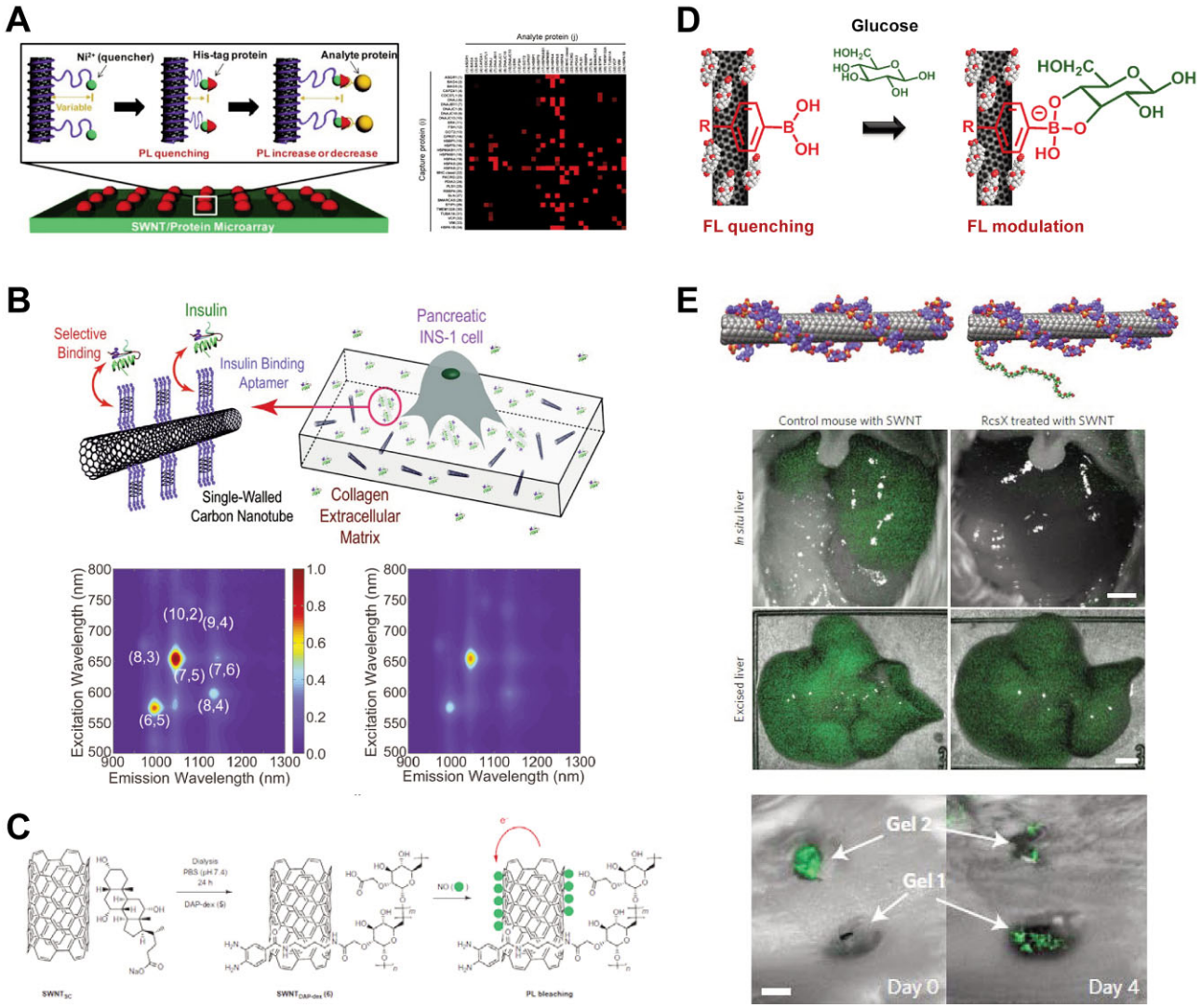

Figure 3. Examples of SWNT-based NIR optical sensors. (**A**) Detection of proteins: schematic of a label-free protein microarray that uses SWNT-based NIR optical sensors and mechanism for signal transduction for label-free detection of protein–protein interactions (left) and heat map of protein–protein interactions between capture protein *i* and analyte protein *j* (34 × 34; right) [81]. (**B**) Detection of insulin: schematic of SWNT-based NIR optical insulin sensors embedded in a collagen extracellular matrix that measure insulin secreted from pancreatic INS-1 cells (top) and photoluminescence excitation spectra of the insulin sensors (bottom) in the absence (left) and presence of insulin (470 µM; right) [77]. (**C**) Detection of NO: preparation of SWNT-based NIR optical NO sensors ($SWNT_{DAP\text{-}dex}$; middle), using diaminophenyl-functionalized dextran (DAP-dex), from SWNTs suspended in sodium cholate ($SWNT_{SC}$; left) and mechanism for NO sensing via photoluminescence (PL) bleaching by NO (right) [66]. (**D**) Detection of glucose: schematic of glucose detection using boronic acid–SWNT complexes via fluorescence (FL) modulation [67]. (**E**) In vivo sensing of NO. SWNT-based NO sensors (top): DNA oligonucleotide $ds(AAAT)_7$ wrapped SWNT (left) and PEG-ligated DNA oligonucleotide $ds(AAAT)_7$ wrapped SWNT (right). In vivo sensor quenching due to inflammation (middle): images of the exposed and excised livers of inflamed (RcsX-treated) and control (healthy) mice 30 min after tail-vein injection of PEG-$(AAAT)_7$ wrapped SWNTs (200 µL injection of 50 mg l^{-1} SWNTs), showing fluorescence quenching in the inflamed mouse. Images of two alginate gels encapsulating SWNT NO sensors, subcutaneously implanted in mouse, showing recovery of the fluorescence on day 4 (bottom) [100]. Reproduced from [66, 67, 77, 81, 100] with permission.

and living cells, in which the conformation change of DNA modulates the fluorescence of SWNTs.

5.2 Detection of proteins

Detecting proteins is important for proteomics and clinical diagnostics [87]. Methods for protein detection include enzyme-linked immunosorbent assays (ELISAs), fluorescence-based protein micro arrays [89, 90], label-free optical methods [91], microcantilevers [92], and nanowire-based field effect transistors [93, 94]. The general goal is to achieve highly sensitive, multiplexed, and label-free detection of proteins [87]. To improve the sensitivity, Chen et al. [87] used functionalized SWNTs as mul-

Table 2. SWNT-based NIR optical biosensors for DNA, proteins, and small molecules

	Sensing platforms and mechanisms	Examples
DNA	DNA-wrapped SWNTs; solvatochromic shift	DNA hybridization [75, 76], single nucleotide polymorphism (SNP) [88], conformational polymorphism [71, 72]
Protein microarrays	Use of functionalized SWNTs as multicolor Raman labels	Protein microarrays (sensitivity down to 1 fM) [87]
	Use of SWNT NIR optical protein sensors in microarrays	Label-free microarray capable of single protein detection [81]; cardiac troponin T detection [95].
	Use of SWNTs conjugated with antibodies as a NIR label for immunoassay	Immunoassay [96]
Insulin	SWNTs functionalized with insulin-binding aptamer	Detect insulin in cellular environments [77]
Hydrogen peroxide (H_2O_2)	SWNT/collagen NIR optical sensor arrays; stochastic quenching	Detect H_2O_2 from living cells down to the single-molecule level [58, 97, 98]
Nitric oxide (NO)	SWNTs functionalized with a diaminophenyl-functionalized dextran [66], ssDNA [60], PEG-ligated DNA [100]; quenching sensors	Detect NO at the single-molecule level [60], in living cells [66, 99], and in mice (in vivo sensing) [100]
ATP	SWNTs combined with a conventional ATP assay; redox-mediated quenching	Detect ATP temporally and spatially in living cells [74]
Porphyrin	DNA aptamer-functionalized SWNTs	Multiplexed detection of plasma porphyrins [78]
Glucose	SWNTs functionalized with glucose oxidase [64], concanavalin A [79], glucose binding protein [80], and boronic acids [67, 111]	SWNT-based NIR optical sensors for glucose monitoring [64, 67, 79, 80, 111]
Genotoxins	DNA-functionalized SWNTs	Multimodal sensing of genotoxins [59]
Nitroaromatics	Peptide-SWNT chaperone sensor	Detect nitroaromatics at the single-molecule level [61]
Riboflavin, thyroxine, oestradiol	Heteropolymer-SWNT complexes; corona phase molecular recognition	Detect riboflavin, thyroxine, and oestradiol [57]
Neurotransmitters	Heteropolymer-SWNT complexes; corona phase molecular recognition	Detect neurotransmitters, including dopamine [73]

ticolor Raman labels in protein microarrays. The sharp Raman scattering peaks of SWNTs and minimal background interference of the Raman signal improved the sensitivity down to 1 fM, a three-order-of-magnitude improvement over typical standard fluorescence-based protein arrays. Another approach is to directly use SWNT-based NIR optical sensors in a microarray for label-free detection of proteins (Fig. 3A) [81]. Using this method, Ahn et al. [81] demonstrated the analysis of a network of 1156 protein–protein interactions in the staurosporine-induced apoptosis of SH-SY5Y cells (Fig. 3A). The single-molecule-level sensitivity of SWNT-based protein sensors decreased the apparent detection limit down to 10 pM for an observation time of 600 s. Zhang et al. [95] also used a similar approach to develop a label-free assay for cardiac troponin T detection, using chitosan-wrapped SWNTs conjugated with troponin antibodies. SWNTs conjugated with antibodies were also used as a NIR label for immunoassay [96].

In addition to proteomics research, Cha et al. [77] developed SWNT-based NIR optical sensors that use an insulin-binding aptamer as a molecular recognition element to detect insulin in cellular environments (Fig. 3B). The sensors selectively modulate the fluorescence of SWNTs upon binding of insulin by using the photo-induced charge transfer between the aptamers and SWNTs. They also demonstrated the detection of insulin secreted by pancreatic cells when stimulated by glucose by embedding the sensors in a collagen extracellular matrix.

5.3 Detection of small molecules

Sensing small molecules is important in understanding various biological processes at the molecular and cellular level. In this section, we present different types of SWNT-based optical sensors for detecting biologically important small molecules down to the single-molecule level [58–60,

97–99]. Detecting reactive oxygen species with spatial resolution in living systems remains challenging, because of their low concentration and short lifetime [97, 98]. To overcome these challenges, Jin et al. [58, 97] developed an array of fluorescent SWNT sensors embedded in a collagen matrix to detect hydrogen peroxide (H_2O_2) molecules. Using the nanosensor array, they measured the signaling flux of H_2O_2 molecules emitted from human epidermal carcinoma cells, stimulated by epidermal growth factor, in real time and with spatial precision. The nanosensor array was also used to measure the efflux of H_2O_2 generated from human umbilical vein endothelial cells at the single-molecule level, when stimulated by vascular endothelial growth factor A and artificial pro-angiogenic factor, europium(III) hydroxide nanorods [98].

Nitric oxide (NO) is another important cellular signaling molecule, involved in diverse biological processes in cardiovascular, nervous, and immune systems [60, 66, 99, 100]. However, detecting NO directly and in real time in biological systems is difficult, because of its large diffusivity and high reactivity with endogenous molecules. To overcome these challenges, Kim et al. [66] developed a SWNT-based NIR optical NO sensor by wrapping SWNTs with a diaminophenyl-functionalized dextran that provides selectivity for NO, in which the binding of NO with the dextran–SWNT complex reversibly bleaches the fluorescence of the SWNT through electron transfer from the top of the SWNT valence band to the lowest unoccupied molecular orbital of NO (Fig. 3C). The sensor could spatiotemporally and reversibly detect NO produced by activating NO synthase in macrophage cells at the nanomolar level. Zhang et al. [60] also demonstrated that a fluorescence-based SWNT sensing array that consists of single-stranded $d(AT)_{15}$ DNA oligonucleotide-wrapped SWNTs selectively detects NO at the single-molecule level. When exposed to NO, the DNA–SWNT complex shows a stepwise decrease of the fluorescence of the SWNTs via exciton quenching, reporting the dynamics of the adsorption and desorption of single NO molecules.

In addition to sensors for hydrogen peroxide and nitric oxide, a SWNT-based NIR optical sensor for adenosine 5′-triphosphate (ATP) was reported [74]. This sensor combines the conventional ATP assay that uses luciferase-mediated bioluminescence with SWNTs, by conjugating luciferases on SWNTs, in which a two-step reaction modulates the fluorescence of SWNTs, involving the detection of ATP and generation of a redox quenching intermediate (oxyluciferin) that quenches the fluorescence of SWNTs. Pan et al. [78] showed a new integrated spectrophotometry- and fluorometry-based sensing method, using SWNTs functionalized with porphyrin-binding DNA aptamers, for multiplexed detection of four porphyrin species (heme, protoporphyrin, coproporphyrin, and uroporphyrin) commonly found in blood. Other examples also include SWNT sensors for genotoxins [59], nitroaromatics [61], and neurotransmitters [73]. Understanding the cellular uptake and intracellular trafficking of SWNTs is important for their intracellular biosensing and other biomedical applications. Given the brevity of this review, we refer interested readers to other references [101–108].

5.4 SWNTs for in vivo sensing

One of the most promising applications of SWNT-based sensors is in vivo sensing. SWNTs have unique optical properties that can solve challenging problems of fluorescence-based in vivo sensing. For example, despite their advantages for in vivo continuous glucose monitoring (e.g., noninvasive sensing), fluorescence-based glucose sensors that use conventional visible fluorophores suffer from lack of optical tissue penetration and photobleaching [36, 109, 110]. To overcome these limitations, researchers have developed prototype SWNT-based NIR optical glucose sensors, showing promising results for long-term in vivo continuous glucose monitoring [36, 38]. For instance, Strano and coworkers demonstrated a series of SWNT-based glucose sensors with various mechanisms to detect glucose, using glucose oxidase [64, 79], concanavalin A [79], glucose binding protein [80], and boronic acids [67, 111] (Fig. 3D). However, SWNT-based optical sensors for in vivo continuous glucose monitoring have not yet been demonstrated.

Despite their unique photostable NIR fluorescence, the use of SWNT-based NIR optical sensors in vivo is challenging. In vivo sensing requires the simultaneous optimization of multiple factors, including molecular recognition, signal transduction, high intensity of the fluorescence signal, biocompatibility, and in vivo stability [36, 100]. Iverson et al. [100] recently reported a reversible and selective detection of NO molecules in mice, using SWNTs conjugated with polyethylene glycol (PEG)-ligated DNA oligonucleotides (Fig. 3E). To address the above-mentioned constraints for in vivo sensing, they synthesized a PEG-ligated DNA oligonucleotide $ds(AAAT)_7$ and wrapped SWNTs with this copolymer, in which the DNA oligonucleotide provides NO selectivity and the PEG moiety provides biocompatibility and stability in vivo, allowing for in vivo circulation of the SWNT complexes. They also demonstrated that the NO sensors encapsulated in alginate can act as an implantable inflammation sensor for NO detection for more than 400 days without intrinsic immune reactivity or other adverse responses (Fig. 3E). This work shows the unique potential of SWNTs for long-term in vivo biosensing.

6 Concluding remarks

We present the recent advances in SWNT-based optical sensing technology for life sciences and biomedicine. Despite great potential of SWNTs for NIR optical biosensing, there are several challenges. A key challenge is to

understand fundamental mechanisms for molecular recognition, signal transduction, and fluorescence modulation of SWNT sensors at the molecular level. For example, a recent study by Zhang et al. [57] that uses corona phase complexes for molecular recognition, highlighted in Section 4, shows a new direction to address this challenge. The design of effective SWNT sensors also requires an understanding of how to effectively transduce molecular recognition into the modulation of the optical signal of SWNTs. Because of the experimental difficulties at the molecular level, numerical modeling and molecular dynamic simulation, combined with experimental studies, can play an important role in this development [57, 112].

The next step of the SWNT sensing technology is to move it from laboratory into biomedical research and clinical use. Although fluorescence-based sensors that use conventional fluorophores have shown high resolution and sensitivity in vitro, the scattering and absorption of optical signal (particularly for visible fluorophores), rapid photobleaching, and strong autofluorescence backgrounds in tissues have limited their use in imaging and sensing in vivo. With their nonphotobleaching NIR fluorescence, SWNTs have shown unique optical properties to overcome these barriers [45]. However, the use of SWNTs for in vivo sensing still requires the simultaneous optimization of multiple factors to achieve both effective sensing and biocompatibility, including molecular recognition, signal transduction, high quantum efficiency, biocompatibility, and in vivo stability [100].

Another important factor for the biomedical applications of SWNTs is their biological safety in the human body [3, 6]. Many studies on the biological applications of SWNTs suggest that the toxicity of SWNTs depends on the surface functionalization of SWNTs and proper functionalization makes them safe as biomaterials [6, 29, 113–116]. For example, SWNTs functionalized with PEGs, injected into the bloodstream of mice, have shown no obvious toxic effects on the mice (evaluated by the necropsy, histology, and blood chemistry measurements) [29, 114]. These studies also showed excretion and clearance of PEG-functionalized SWNTs from mice via biliary and renal pathways. However, the future use of SWNT-based sensors in biomedicine requires further systematic and thorough studies on the toxicity of SWNTs.

The in vivo kinetics of SWNTs is another important factor to understand, including how SWNTs circulate in the body, whether they accumulate in specific organs, and whether or not and how they are cleared from the body [6, 29, 49, 113–115]. Independent studies suggest that the in vivo kinetics of SWNTs depends on surface functionalization, such as the length and structure of functionalizing molecules [29, 113–116]. A study with individualized, chemically pristine SWNTs, initially dispersed with surfactant Pluronic F108, displaced with blood proteins after being intravenously administrated to rabbits, showed a half-life of the SWNTs of 1 h in the blood stream and significant accumulation of the SWNTs in the liver (as other nanomaterials) [113]. Another study with SWNTs functionalized with branched PEG chains, intravenously injected into mice, showed the circulation of the SWNTs in the blood stream for up to 1 day, dominant yet relatively low uptake in the reticuloendothelial system (RES) (i.e., liver and spleen), and near-complete clearance from the main organs in 2 months [29]. This study also showed that SWNTs functionalized with longer and more branched PEGs show longer blood circulation and lower uptake in the RES [29].

Additionally, these translational efforts require standard procedures to prepare well-characterized, high purity SWNTs, as the length, degree of aggregation, surface functionalization, and impurities in SWNTs affect their toxicity. For instance, ultrapure carbon materials used inside the human body, such as artificial heart valves, artificial finger joints, and black tattoos, containing nanoscale pure carbon black, have not reported safety concerns [6]. Continuous research will overcome these challenges and realize the full potential of SWNTs as NIR optical biosensors that can solve challenging problems in life sciences and biomedicine.

The authors declare no commercial or financial conflict of interest.

Kyungsuk Yum is assistant professor in the department of materials science and engineering at the University of Texas, Arlington. He is also a faculty affiliate of the biomedical engineering program of UT Arlington, UT Dallas, and UT Southwestern Medical Center. He received his PhD in Mechanical Science and Engineering from the University of Illinois at Urbana-Champaign (UIUC). Before joining the University of Texas, he worked as a postdoctoral research associate in chemical engineering at MIT and in bioengineering at UC Berkeley. His research interests are biologically inspired materials and engineering systems, nanobiotechnology, and nano-biomanufacturing.

7 References

[1] Kim, B. Y. S., Rutka, J. T., Chan, W. C. W., Nanomedicine. *N. Engl. J. Med.* 2010, *363*, 2434–2443.
[2] Liu, Z., Tabakman, S., Welsher, K., Dai, H., Carbon nanotubes in biology and medicine: In vitro and in vivo detection, imaging and drug delivery. *Nano Res.* 2009, *2*, 85–120.
[3] Kostarelos, K., Bianco, A., Prato, M., Promises, facts and challenges for carbon nanotubes in imaging and therapeutics. *Nat. Nanotechnol.* 2009, *4*, 627–633.

[4] Boghossian, A. A., Zhang, J., Barone, P. W., Reuel, N. F., et al., Near-infrared fluorescent sensors based on single-walled carbon nanotubes for life sciences applications. *ChemSusChem* 2011, *4*, 848–863.
[5] Kruss, S., Hilmer, A. J., Zhang, J., Reuel, N. F., et al., Carbon nanotubes as optical biomedical sensors. *Adv. Drug Delivery Rev.* 2013, *65*, 1933–1950.
[6] Saito, N., Haniu, H., Usui, Y., Aoki, K., et al., Safe clinical use of carbon nanotubes as innovative biomaterials. *Chem. Rev.* 2014, *114*, 6040–6079.
[7] Iijima, S., Helical microtubules of graphitic carbon. *Nature* 1991, *354*, 56–58.
[8] Odom, T. W., Huang, J.-L., Kim, P., Lieber, C. M., Atomic structure and electronic properties of single-walled carbon nanotubes. *Nature* 1998, *391*, 62–64.
[9] Ajayan, P., Nanotubes from carbon. *Chem. Rev.* 1999, *99*, 1787–1800.
[10] Tans, S. J., Devoret, M. H., Dai, H., Thess, A., et al., Individual single-wall carbon nanotubes as quantum wires. *Nature* 1997, *386*, 474–477.
[11] O'Connell, M. J., Bachilo, S. M., Huffman, C. B., Moore, V. C., et al., Band gap fluorescence from individual single-walled carbon nanotubes. *Science* 2002, *297*, 593–596.
[12] Bachilo, S. M., Strano, M. S., Kittrell, C., Hauge, R. H., et al., Structure-assigned optical spectra of single-walled carbon nanotubes. *Science* 2002, *298*, 2361–2366.
[13] Ghosh, S., Bachilo, S. M., Weisman, R. B., Advanced sorting of single-walled carbon nanotubes by nonlinear density-gradient ultracentrifugation. *Nat. Nanotechnol.* 2010, *5*, 443–450.
[14] Zhou, J., Wang, C., Qian, Z., Chen, C., et al., Highly efficient fluorescent multi-walled carbon nanotubes functionalized with diamines and amides. *J. Mater. Chem.* 2012, *22*, 11912–11914.
[15] Li, H., Tian, J., Wang, L., Zhang, Y., Sun, X., Multi-walled carbon nanotubes as an effective fluorescent sensing platform for nucleic acid detection. *J. Mater. Chem.* 2011, *21*, 824–828.
[16] Pantarotto, D., Singh, R., McCarthy, D., Erhardt, M., et al., Functionalized carbon nanotubes for plasmid DNA gene delivery. *Angew. Chem. Int. Ed.* 2004, *43*, 5242–5246.
[17] Liu, Y., Wu, D.-C., Zhang, W.-D., Jiang, X., et al., Polyethylenimine-grafted multiwalled carbon nanotubes for secure noncovalent immobilization and efficient delivery of DNA. *Angew. Chem., Int. Ed.* 2005, *44*, 4782–4785.
[18] Singh, R., Pantarotto, D., McCarthy, D., Chaloin, O., et al., Binding and condensation of plasmid DNA onto functionalized carbon nanotubes:? Toward the construction of nanotube-based gene delivery vectors. *J. Am. Chem. Soc.* 2005, *127*, 4388–4396.
[19] Wu, H.-C., Chang, X., Liu, L., Zhao, F., Zhao, Y., Chemistry of carbon nanotubes in biomedical applications. *J. Mater. Chem.* 2010, *20*, 1036–1052.
[20] Chen, X., Kis, A., Zettl, A., Bertozzi, C. R., A cell nanoinjector based on carbon nanotubes. *Proc. Natl. Acad. Sci. USA* 2007, *104*, 8218–8222.
[21] Yum, K., Na, S., Xiang, Y., Wang, N., Yu, M.-F., Mechanochemical delivery and dynamic tracking of fluorescent quantum dots in the cytoplasm and nucleus of living cells. *Nano Lett.* 2009, *9*, 2193–2198.
[22] Yum, K., Wang, N., Yu, M.-F., Nanoneedle: A multifunctional tool for biological studies in living cells. *Nanoscale* 2010, *2*, 363–372.
[23] Wang, F., Dukovic, G., Brus, L. E., Heinz, T. F., The optical resonances in carbon nanotubes arise from excitons. *Science* 2005, *308*, 838–841.
[24] Avouris, P., Freitag, M., Perebeinos, V., Carbon-nanotube photonics and optoelectronics. *Nat. Photon.* 2008, *2*, 341–350.
[25] Luer, L., Hoseinkhani, S., Polli, D., Crochet, J., et al., Size and mobility of excitons in (6, 5) carbon nanotubes. *Nat. Phys.* 2009, *5*, 54–58.
[26] Cognet, L., Tsyboulski, D. A., Rocha, J.-D. R., Doyle, C. D., et al., Stepwise quenching of exciton fluorescence in carbon nanotubes by single-molecule reactions. *Science* 2007, *316*, 1465–1468.
[27] Siitonen, A. J., Tsyboulski, D. A., Bachilo, S. M., Weisman, R. B., Surfactant-dependent exciton mobility in single-walled carbon nanotubes studied by single-molecule reactions. *Nano Lett.* 2010, *10*, 1595–1599.
[28] Heller, D. A., Baik, S., Eurell, T. E., Strano, M. S., Single–walled carbon nanotube spectroscopy in live cells: Towards long–term labels and optical sensors. *Adv. Mater.* 2005, *17*, 2793–2799.
[29] Liu, Z., Davis, C., Cai, W., He, L., et al., Circulation and long-term fate of functionalized, biocompatible single-walled carbon nanotubes in mice probed by Raman spectroscopy. *Proc. Natl. Acad. Sci. USA* 2008, *105*, 1410–1415.
[30] Zavaleta, C., de la Zerda, A., Liu, Z., Keren, S., et al., Noninvasive Raman spectroscopy in living mice for evaluation of tumor targeting with carbon nanotubes. *Nano Lett.* 2008, *8*, 2800–2805.
[31] Keren, S., Zavaleta, C., Cheng, Z., de la Zerda, A., et al., Noninvasive molecular imaging of small living subjects using Raman spectroscopy. *Proc. Natl. Acad. Sci. USA* 2008, *105*, 5844–5849.
[32] Liu, Z., Tabakman, S., Sherlock, S., Li, X., et al., Multiplexed five-color molecular imaging of cancer cells and tumor tissues with carbon nanotube Raman tags in the near-infrared. *Nano Res.* 2010, *3*, 222–233.
[33] Gong, H., Peng, R., Liu, Z., Carbon nanotubes for biomedical imaging: The recent advances. *Adv. Drug Delivery Rev.* 2013, *65*, 1951–1963.
[34] Rao, A. M., Richter, E., Bandow, S., Chase, B., et al., Diameter-selective Raman scattering from vibrational modes in carbon nanotubes. *Science* 1997, *275*, 187–191.
[35] Welsher, K., Sherlock, S. P., Dai, H., Deep-tissue anatomical imaging of mice using carbon nanotube fluorophores in the second near-infrared window. *Proc. Natl. Acad. Sci. USA* 2011, *108*, 8943–8948.
[36] Yum, K., McNicholas, T. P., Mu, B., Strano, M. S., Single-walled carbon nanotube-based near-infrared optical glucose sensors toward in vivo continuous glucose monitoring. *J. Diabetes Sci. Technol.* 2013, *7*, 72–87.
[37] Hartschuh, A., Pedrosa, H. N., Novotny, L., Krauss, T. D., Simultaneous fluorescence and Raman scattering from single carbon nanotubes. *Science* 2003, *301*, 1354–1356.
[38] Barone, P. W., Parker, R. S., Strano, M. S., In vivo fluorescence detection of glucose using a single-walled carbon nanotube optical sensor:? Design, fluorophore properties, advantages, and disadvantages. *Anal. Chem.* 2005, *77*, 7556–7562.
[39] Ju, S.-Y., Kopcha, W. P., Papadimitrakopoulos, F., Brightly fluorescent single-walled carbon nanotubes via an oxygen-excluding surfactant organization. *Science* 2009, *323*, 1319–1323.
[40] Miyauchi, Y., Iwamura, M., Mouri, S., Kawazoe, T., et al., Brightening of excitons in carbon nanotubes on dimensionality modification. *Nat. Photon.* 2013, *7*, 715–719.
[41] Piao, Y., Meany, B., Powell, L. R., Valley, N., et al., Brightening of carbon nanotube photoluminescence through the incorporation of sp3 defects. *Nat. Chem.* 2013, *5*, 840–845.
[42] Bashkatov, A. N., Genina, E. A., Kochubey, V. I., Tuchin, V. V., Optical properties of human skin, subcutaneous and mucous tissues in the wavelength range from 400 to 2000 nm. *J. Phys. D: Appl. Phys.* 2005, *38*, 2543–2555.
[43] Troy, T. L., Thennadil, S. N., Optical properties of human skin in the near infrared wavelength range of 1000 to 2200 nm. *J. of Biomed. Opt.* 2001, *6*, 167–176.
[44] Lim, Y. T., Kim, S., Nakayama, A., Stott, N. E., et al., Selection of quantum dot wavelengths for biomedical assays and imaging. *Mol. Imag.* 2003, *2*, 50–64.

[45] Hong, G., Lee, J. C., Robinson, J. T., Raaz, U., et al., Multifunctional in vivo vascular imaging using near-infrared II fluorescence. *Nat. Med.* 2012, *18*, 1841–1846.
[46] Smith, A. M., Mancini, M. C., Nie, S., Bioimaging: Second window for in vivo imaging. *Nat. Nanotechnol.* 2009, *4*, 710–711.
[47] Terentyuk, G. S., Maslyakova, G. N., Suleymanova, L. V., Khlebtsov, N. G., et al., Laser-induced tissue hyperthermia mediated by gold nanoparticles: Toward cancer phototherapy. *J. of Biomed. Opt.* 2009, *14*, 021016-021016-021019.
[48] Welsher, K., Liu, Z., Sherlock, S. P., Robinson, J. T., et al., A route to brightly fluorescent carbon nanotubes for near-infrared imaging in mice. *Nat. Nanotechnol.* 2009, *4*, 773–780.
[49] Liu, Z., Cai, W., He, L., Nakayama, N., et al., In vivo biodistribution and highly efficient tumour targeting of carbon nanotubes in mice. *Nat. Nanotechnol.* 2007, *2*, 47–52.
[50] Robinson, J., Welsher, K., Tabakman, S., Sherlock, S., et al., High performance in vivo near-IR (>1 μm) imaging and photothermal cancer therapy with carbon nanotubes. *Nano Res.* 2010, *3*, 779–793.
[51] Diao, S., Hong, G., Robinson, J. T., Jiao, L., et al., Chirality enriched (12,1) and (11,3) single-walled carbon nanotubes for biological imaging. *J. Am. Chem. Soc.* 2012, *134*, 16971–16974.
[52] Antaris, A. L., Robinson, J. T., Yaghi, O. K., Hong, G., et al., Ultra-low doses of chirality sorted (6, 5) carbon nanotubes for simultaneous tumor imaging and photothermal therapy. *ACS Nano* 2013, *7*, 3644–3652.
[53] Smith, B. R., Zavaleta, C., Rosenberg, J., Tong, R., et al., High-resolution, serial intravital microscopic imaging of nanoparticle delivery and targeting in a small animal tumor model. *Nano Today* 2013, *8*, 126–137.
[54] Ghosh, D., Bagley, A. F., Na, Y. J., Birrer, M. J., et al., Deep, noninvasive imaging and surgical guidance of submillimeter tumors using targeted M13-stabilized single-walled carbon nanotubes. *Proc. Natl. Acad. Sci. USA* 2014, *111*, 13948–13953.
[55] Yi, H., Ghosh, D., Ham, M.-H., Qi, J., et al., M13 phage-functionalized single-walled carbon nanotubes as nanoprobes for second near-infrared window fluorescence imaging of targeted tumors. *Nano Lett.* 2012, *12*, 1176–1183.
[56] Singh, R., Torti, S. V., Carbon nanotubes in hyperthermia therapy. *Adv. Drug Delivery Rev.* 2013, *65*, 2045–2060.
[57] Zhang, J., Landry, M. P., Barone, P. W., Kim, J.-H., et al., Molecular recognition using corona phase complexes made of synthetic polymers adsorbed on carbon nanotubes. *Nat. Nanotechnol.* 2013, *8*, 959–968.
[58] Jin, H., Heller, D. A., Kim, J.-H., Strano, M. S., Stochastic analysis of stepwise fluorescence quenching reactions on single-walled carbon nanotubes: Single molecule sensors. *Nano Lett.* 2008, *8*, 4299–4304.
[59] Heller, D. A., Jin, H., Martinez, B. M., Patel, D., et al., Multimodal optical sensing and analyte specificity using single-walled carbon nanotubes. *Nat. Nanotechnol.* 2009, *4*, 114–120.
[60] Zhang, J., Boghossian, A. A., Barone, P. W., Rwei, A., et al., Single molecule detection of nitric oxide enabled by $d(AT)_{15}$ DNA adsorbed to near infrared fluorescent single-walled carbon nanotubes. *J. Am. Chem. Soc.* 2010, *133*, 567–581.
[61] Heller, D. A., Pratt, G. W., Zhang, J., Nair, N., et al., Peptide secondary structure modulates single-walled carbon nanotube fluorescence as a chaperone sensor for nitroaromatics. *Proc. Natl. Acad. Sci. USA* 2011, *108*, 8544–8549.
[62] Strano, M. S., Huffman, C. B., Moore, V. C., O'Connell, M. J., et al., Reversible, band-gap-selective protonation of single-walled carbon nanotubes in solution. *J. Phys. Chem. B* 2003, *107*, 6979–6985.
[63] O'Connell, M. J., Eibergen, E. E., Doorn, S. K., Chiral selectivity in the charge-transfer bleaching of single-walled carbon-nanotube spectra. *Nat. Mater.* 2005, *4*, 412–418.
[64] Barone, P. W., Baik, S., Heller, D. A., Strano, M. S., Near-infrared optical sensors based on single-walled carbon nanotubes. *Nat. Mater.* 2005, *4*, 86–92.
[65] Satishkumar, B. C., Brown, L. O., Gao, Y., Wang, C.-C., et al., Reversible fluorescence quenching in carbon nanotubes for biomolecular sensing. *Nat. Nanotechnol.* 2007, *2*, 560–564.
[66] Kim, J.-H., Heller, D. A., Jin, H., Barone, P. W., et al., The rational design of nitric oxide selectivity in single-walled carbon nanotube near-infrared fluorescence sensors for biological detection. *Nat. Chem.* 2009, *1*, 473–481.
[67] Yum, K., Ahn, J.-H., McNicholas, T. P., Barone, P. W., et al., Boronic acid library for selective, reversible near-infrared fluorescence quenching of surfactant suspended single-walled carbon nanotubes in response to glucose. *ACS Nano* 2012, *6*, 819–830.
[68] Choi, J. H., Strano, M. S., Solvatochromism in single-walled carbon nanotubes. *Appl. Phys. Lett.* 2007, *90*, 223114.
[69] Walsh, A. G., Vamivakas, A. N., Yin, Y., Cronin, S. B., et al., Screening of excitons in single, suspended carbon nanotubes. *Nano Lett.* 2007, *7*, 1485–1488.
[70] Silvera-Batista, C. A., Wang, R. K., Weinberg, P., Ziegler, K. J., Solvatochromic shifts of single-walled carbon nanotubes in nonpolar microenvironments. *Phys. Chem. Chem. Phys.* 2010, *12*, 6990–6998.
[71] Heller, D. A., Jeng, E. S., Yeung, T.-K., Martinez, B. M., et al., Optical detection of DNA conformational polymorphism on single-walled carbon nanotubes. *Science* 2006, *311*, 508–511.
[72] Jin, H., Jeng, E. S., Heller, D. A., Jena, P. V., et al., Divalent ion and thermally induced DNA conformational polymorphism on single-walled carbon nanotubes. *Macromolecules* 2007, *40*, 6731–6739.
[73] Kruss, S., Landry, M. P., Vander Ende, E., Lima, B. M. A., et al., Neurotransmitter detection using corona phase molecular recognition on fluorescent single-walled carbon nanotube sensors. *J. Am. Chem. Soc.* 2013, *136*, 713–724.
[74] Kim, J.-H., Ahn, J.-H., Barone, P. W., Jin, H., et al., A luciferase/single-walled carbon nanotube conjugate for near-infrared fluorescent detection of cellular ATP. *Angew. Chem. Int. Ed.* 2010, *49*, 1456–1459.
[75] Jeng, E. S., Moll, A. E., Roy, A. C., Gastala, J. B., Strano, M. S., Detection of DNA hybridization using the near-infrared band-gap fluorescence of single-walled carbon nanotubes. *Nano Lett.* 2006, *6*, 371–375.
[76] Jeng, E. S., Barone, P. W., Nelson, J. D., Strano, M. S., Hybridization kinetics and thermodynamics of DNA adsorbed to individually dispersed single walled carbon nanotubes. *Small* 2007, *3*, 1602–1609.
[77] Cha, T.-G., Baker, B. A., Sauffer, M. D., Salgado, J., et al., Optical nanosensor architecture for cell-signaling molecules using DNA aptamer-coated carbon nanotubes. *ACS Nano* 2011, *5*, 4236–4244.
[78] Pan, J., Zhang, H., Cha, T.-G., Chen, H., Choi, J. H., Multiplexed optical detection of plasma porphyrins using DNA aptamer-functionalized carbon nanotubes. *Anal. Chem.* 2013, *85*, 8391–8396.
[79] Barone, P. W., Strano, M. S., Reversible control of carbon nanotube aggregation for a glucose affinity sensor. *Angew. Chem. Int. Ed.* 2006, *45*, 8138–8141.
[80] Yoon, H., Ahn, J.-H., Barone, P. W., Yum, K., et al., Periplasmic binding proteins as optical modulators of single-walled carbon nanotube fluorescence: Amplifying a nanoscale actuator. *Angew. Chem. Int. Ed.* 2011, *50*, 1828–1831.
[81] Ahn, J.-H., Kim, J.-H., Reuel, N. F., Barone, P. W., et al., Label-free, single protein detection on a near-infrared fluorescent single-walled carbon nanotube/protein microarray fabricated by cell-free synthesis. *Nano Lett.* 2011, *11*, 2743–2752.
[82] Liu, H., Nishide, D., Tanaka, T., Kataura, H., Large-scale single-chirality separation of single-wall carbon nanotubes by simple gel chromatography. *Nat. Commun.* 2011, *2*, 309.

[83] Liu, J., Wang, C., Tu, X., Liu, B., et al., Chirality-controlled synthesis of single-wall carbon nanotubes using vapour-phase epitaxy. *Nat. Commun.* 2012, *3*, 1199.
[84] Liu, H., Tanaka, T., Urabe, Y., Kataura, H., High-efficiency single-chirality separation of carbon nanotubes using temperature-controlled gel chromatography. *Nano Lett.* 2013, *13*, 1996–2003.
[85] Fagan, J. A., Khripin, C. Y., Silvera Batista, C. A., Simpson, J. R., et al., Isolation of specific small-diameter single-wall carbon nanotube species via aqueous two-phase extraction. *Adv. Mater.* 2014, *26*, 2800–2804.
[86] Jain, R. M., Tvrdy, K., Han, R., Ulissi, Z., Strano, M. S., Quantitative theory of adsorptive separation for the electronic sorting of single-walled carbon nanotubes. *ACS Nano* 2014, *8*, 3367–3379.
[87] Chen, Z., Tabakman, S. M., Goodwin, A. P., Kattah, M. G., et al., Protein microarrays with carbon nanotubes as multicolor Raman labels. *Nat. Biotechnol.* 2008, *26*, 1285–1292.
[88] Jeng, E. S., Nelson, J. D., Prather, K. L. J., Strano, M. S., Detection of a single nucleotide polymorphism using single-walled carbon-nanotube near-infrared fluorescence. *Small* 2010, *6*, 40–43.
[89] MacBeath, G., Schreiber, S. L., Printing proteins as microarrays for high-throughput function determination. *Science* 2000, *289*, 1760–1763.
[90] Bailey, R. C., Kwong, G. A., Radu, C. G., Witte, O. N., Heath, J. R., DNA-encoded antibody libraries:? A unified platform for multiplexed cell sorting and detection of genes and proteins. *J. Am. Chem. Soc.* 2007, *129*, 1959–1967.
[91] Landry, J. P., Zhu, X. D., Gregg, J. P., Label-free detection of microarrays of biomolecules by oblique-incidence reflectivity difference microscopy. *Opt. Lett.* 2004, *29*, 581–583.
[92] Wu, G., Datar, R. H., Hansen, K. M., Thundat, T., et al., Bioassay of prostate-specific antigen (PSA) using microcantilevers. *Nat. Biotechnol.* 2001, *19*, 856–860.
[93] Kong, J., Franklin, N. R., Zhou, C., Chapline, M. G., et al., Nanotube molecular wires as chemical sensors. *Science* 2000, *287*, 622–625.
[94] Zheng, G., Patolsky, F., Cui, Y., Wang, W. U., Lieber, C. M., Multiplexed electrical detection of cancer markers with nanowire sensor arrays. *Nat. Biotechnol.* 2005, *23*, 1294–1301.
[95] Zhang, J., Kruss, S., Hilmer, A. J., Shimizu, S., et al., A rapid, direct, quantitative, and label-free detector of cardiac biomarker troponin T using near-infrared fluorescent single-walled carbon nanotube sensors. *Adv. Healthcare Mater.* 2014, *3*, 412–423.
[96] Iizumi, Y., Okazaki, T., Ikehara, Y., Ogura, M., et al., Immunoassay with single-walled carbon nanotubes as near-infrared fluorescent labels. *ACS Appl. Mater. Interfaces* 2013, *5*, 7665–7670.
[97] Jin, H., Heller, D. A., Kalbacova, M., Kim, J.-H., et al., Detection of single-molecule H_2O_2 signalling from epidermal growth factor receptor using fluorescent single-walled carbon nanotubes. *Nat. Nanotechnol.* 2010, *5*, 302–309.
[98] Kim, J.-H., Patra, C. R., Arkalgud, J. R., Boghossian, A. A., et al., Single-molecule detection of H_2O_2 mediating angiogenic redox signaling on fluorescent single-walled carbon nanotube array. *ACS Nano* 2011, *5*, 7848–7857.
[99] Ulissi, Z. W., Sen, F., Gong, X., Sen, S., et al., Spatiotemporal intracellular nitric oxide signaling captured using internalized, near-infrared fluorescent carbon nanotube nanosensors. *Nano Lett.* 2014, *14*, 4887–4894.
[100] Iverson, N. M., Barone, P. W., Shandell, M., Trudel, L. J., et al., In vivo biosensing via tissue-localizable near-infrared-fluorescent single-walled carbon nanotubes. *Nat. Nanotechnol.* 2013, *8*, 873–880.
[101] Cherukuri, P., Bachilo, S. M., Litovsky, S. H., Weisman, R. B., Near-infrared fluorescence microscopy of single-walled carbon nanotubes in phagocytic cells. *J. Am. Chem. Soc.* 2004, *126*, 15638–15639.
[102] Kam, N. W. S., Liu, Z., Dai, H., Carbon nanotubes as intracellular transporters for proteins and DNA: An investigation of the uptake mechanism and pathway. *Angew. Chem. Int. Ed.* 2006, *45*, 577–581.
[103] Kostarelos, K., Lacerda, L., Pastorin, G., Wu, W., et al., Cellular uptake of functionalized carbon nanotubes is independent of functional group and cell type. *Nat. Nanotechnol.* 2007, *2*, 108.
[104] Jin, H., Heller, D. A., Strano, M. S., Single-particle tracking of endocytosis and exocytosis of single-walled carbon nanotubes in NIH-3T3 cells. *Nano Lett.* 2008, *8*, 1577-1585.
[105] Jin, H., Heller, D. A., Sharma, R., Strano, M. S., Size-dependent cellular uptake and expulsion of single-walled carbon nanotubes: Single particle tracking and a generic uptake model for nanoparticles. *ACS Nano* 2009, *3*, 149–158.
[106] Iversen, T.-G., Skotland, T., Sandvig, K., Endocytosis and intracellular transport of nanoparticles: Present knowledge and need for future studies. *Nano Today* 2011, *6*, 176–185.
[107] Hong, G., Wu, J. Z., Robinson, J. T., Wang, H., et al., Three-dimensional imaging of single nanotube molecule endocytosis on plasmonic substrates. *Nat. Commun.* 2012, *3*, 700.
[108] Donkor, D. A., Tang, X. S., Tube length and cell type-dependent cellular responses to ultra-short single-walled carbon nanotube. *Biomaterials* 2014, *35*, 3121–3131.
[109] Steiner, M.-S., Duerkop, A., Wolfbeis, O. S., Optical methods for sensing glucose. *Chem. Soc. Rev.* 2011, *40*, 4805–4839.
[110] Pickup, J. C., Hussain, F., Evans, N. D., Rolinski, O. J., Birch, D. J. S., Fluorescence-based glucose sensors. *Biosens. Bioelectron.* 2005, *20*, 2555–2565.
[111] Mu, B., McNicholas, T. P., Zhang, J., Hilmer, A. J., et al., A structure–function relationship for the optical modulation of phenyl boronic acid-grafted, polyethylene glycol-wrapped single-walled carbon nanotubes. *J. Am. Chem. Soc.* 2012, *134*, 17620–17627.
[112] Lin, S., Zhang, J., Strano, M. S., Blankschtein, D., Understanding selective molecular recognition in integrated carbon nanotube-polymer sensors by simulating physical analyte binding on carbon nanotube-polymer scaffolds. *Soft Matter* 2014, *10*, 5991–6004.
[113] Cherukuri, P., Gannon, C. J., Leeuw, T. K., Schmidt, H. K., et al., Mammalian pharmacokinetics of carbon nanotubes using intrinsic near-infrared fluorescence. *Proc. Natl. Acad. Sci. USA* 2006, *103*, 18882–18886.
[114] Schipper, M. L., Nakayama-Ratchford, N., Davis, C. R., Kam, N. W. S., et al., A pilot toxicology study of single-walled carbon nanotubes in a small sample of mice. *Nat. Nanotechnol.* 2008, *3*, 216–221.
[115] Ge, C., Du, J., Zhao, L., Wang, L., et al., Binding of blood proteins to carbon nanotubes reduces cytotoxicity. *Proc. Natl. Acad. Sci. USA* 2011, *108*, 16968–16973.
[116] Robinson, J. T., Hong, G., Liang, Y., Zhang, B., et al., In vivo fluorescence imaging in the second near-infrared window with long circulating carbon nanotubes capable of ultrahigh tumor uptake. *J. Am. Chem. Soc.* 2012, *134*, 10664–10669.